Environmental Science & Technology

Article

pubs.acs.org/est

Manganese Peroxidase Degrades Pristine but Not Surface-Oxidized (Carboxylated) Single-Walled Carbon Nanotubes

Chengdong Zhang,*[,†] Wei Chen,[†] and Pedro J. J. Alvarez*[,‡]

[†]College of Environmental Science and Engineering/Ministry of Education Key Laboratory of Pollution Processes and Environmental Criteria/Tianjin Key Laboratory of Environmental Remediation and Pollution Control, Nankai University, Tianjin 300071, People's Republic of China

[‡]Department of Civil and Environmental Engineering, Rice University, Houston, Texas 77005, United States

Supporting Information

ABSTRACT: The transformation of engineered nanomaterials in the environment can significantly affect their transport, fate, bioavailability, and toxicity. Little is known about the biotransformation potential of single-walled carbon nanotubes (SWNTs). In this study, we compared the enzymatic transformation of SWNTs and oxidized (carboxylated) SWNTs (O-SWNTs) using three ligninolytic enzymes: lignin peroxidase, manganese peroxidase (MnP), and laccase. Only MnP was capable of transforming SWNTs, as determined by Raman spectroscopy, near-infrared spectroscopy, and transmission electron microscopy. Interestingly, MnP degraded SWNTs but not O-SWNTs. The recalcitrance of O-SWNTs to enzymatic transformation is likely attributable to the binding of Mn^{2+} by their surface carboxyl groups at the enzyme binding site, which inhibits critical steps in the MnP catalytic cycle (i.e., Mn^{2+} oxidation and Mn^{3+} dissociation from the enzyme). Our results suggest that oxygen-containing surface functionalities do not necessarily facilitate the biodegradation of carbonaceous nanomaterials, as is commonly assumed.

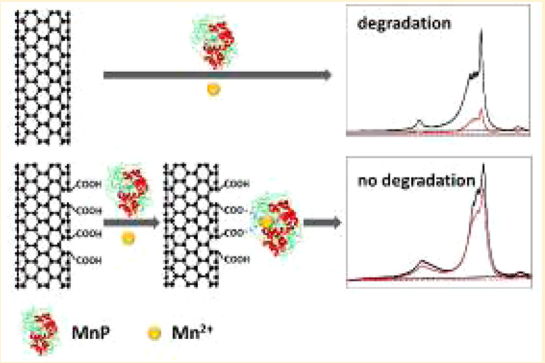

INTRODUCTION

Carbon nanotubes (CNTs) have attracted increasing attention because of their unique electrical, optical, and mechanical properties.[1] Single-walled carbon nanotubes (SWNTs) are particularly attractive for potential applications in electronics,[2] biomedical engineering,[3] drug delivery,[4] biosensor technology,[5] and water treatment.[6] The rapid growth in the production and use of SWNTs has raised concerns about their potential unintended impacts associated with their toxicity and potential interactions with environmental contaminants.[7−9]

Transformations of engineered nanomaterials in the environment can significantly alter their transport, fate, bioavailability, and toxicity.[10,11] While the high diversity of microorganisms and enzymes capable of transforming relatively recalcitrant organic compounds in the environment suggests that the biotransformation of CNTs is possible, these reactions are poorly understood. Three studies have reported the enzymatic transformation of oxidized SWNTs (O-SWNTs), whereas no transformation of pristine SWNTs was observed under identical conditions. Allen et al.[12,13] reported the degradation of O-SWNTs by horseradish peroxidase (HRP) in the presence of 40 μM H_2O_2 and proposed that the reactive oxygen species (ROS) generated through the heterolytic cleavage of H_2O_2 (e.g., $^{\bullet}OH$ and $^{\bullet}OOH$) were responsible for this degradation. Kagan et al.[14] demonstrated that human myeloperoxidase (hMPO) could catalyze the degradation of O-SWNTs. Reactive radical intermediates of hMPO and hypochlorite (e.g., $NO^{\bullet}$ and $ONOO^-$) were proposed as the pertinent oxidants. These results underscore the possibility that CNTs can be degraded (or surface-altered) by enzymatic reactions and suggest that other peroxidases might be able to catalyze similar reactions.

Other enzymes of potential interest for CNT biodegradation include ligninolytic heme peroxidases, such as manganese peroxidase (MnP) and lignin peroxidase (LiP). Similarly to HRP, these enzymes have broad substrate specificities and strong oxidizing capacities and have been reported to degrade relatively recalcitrant compounds, such as lignin and polycyclic aromatic hydrocarbons.[15−17] Ligninolytic enzymes have also been implicated in the fungal metabolism of fullerol,[18] suggesting the possibility that such enzymes might also transform CNTs.

Surface O functionalities may influence the susceptibility of CNTs to enzymatic transformation. For example, negatively charged O-SWNTs have been reported to orient themselves (through carboxyl groups) toward a positively charged arginine residue near the heme site of HRP, while pristine SWNTs orient themselves at the distal end of the enzyme away from the

Received: March 5, 2014
Revised: June 15, 2014
Accepted: June 20, 2014
Published: June 20, 2014

dx.doi.org/10.1021/es5011175 | Environ. Sci. Technol. 2014, 48, 7918−7923

active heme site and are thus not transformed by this enzyme.[13] Furthermore, functionalization and defects on SWNT surfaces may facilitate subsequent oxidation.[19] Accordingly, the degradation of carboxylated SWNTs in a phagolysosomal simulant (consisting of Na_2HPO_4, NaCl, Na_2SO_4, $CaCl_2$, glycine, and potassium hydrogen phthalate buffer salts) was observed, whereas pristine SWNTs were not degraded under the same conditions.[19] Acid carboxylation not only introduced −COOH surface groups but also damaged the tubular graphitic backbone and, thus, created defects that were easier to attack, enhancing degradation. Therefore, it is generally believed that surface functionalization, in particular, carboxylation, facilitates enzymatic degradation.

In this study, we reconsidered this paradigm by comparing the capability of three ligninolytic enzymes, LiP, MnP, and laccase (Lac), to transform SWNTs and O-SWNTs. Different analytical methods, including transmission electron microscopy (TEM), Raman spectroscopy, and near-infrared spectroscopy (NIR), were used to provide mechanistic insights into the effects of functionalization on CNT susceptibility to enzymatic transformation.

MATERIALS AND METHODS

Materials. LiP (E.C. 1.11.1.14, Cat. 42603), MnP (E.C. 1.11.1.13, from white-rot fungus *Phanerochaete chrysosporium*), Lac (E.C.1.10.3.2, from *Trametes versicolor*), H_2O_2, $MnSO_4$, and 2,2′-azino-bis(3-ethylbenzthiazoline-6-sulfonate) (ABTS) were purchased from Sigma−Aldrich. SWNTs (P2-SWNTs) and O-SWNTs (P3-SWNTs) were purchased from Carbon Solution, Inc. (Riverside, CA). The physicochemical properties of the CNTs are shown in Table 1. The CNTs were characterized by

Table 1. Physicochemical Properties of SWNTs and O-SWNTs

	diameter[a] (nm)	length[a] (μm)	C[b] (%, w/w)	O[b] (%, w/w)
SWNTs	∼4−5	∼1.0	94.3	5.7
O-SWNTs	∼4−5	∼1.0	90.3	9.7

[a]From product information of the manufacturer. [b]Determined by XPS analysis.

TEM, X-ray photoelectron spectroscopy (XPS), and thermogravimetric analysis (TGA). XPS analysis was conducted in an ultrahigh-vacuum system equipped with a SPECS LHS-10 hemispherical electron analyzer. For TGA analysis (Q50, TA Instruments, New Castle, DE), the temperature was ramped from room temperature to 850 °C at 5 °C/min under a N_2 atmosphere. The diameters of the SWNTs and O-SWNTs were about 4−5 nm based on TEM analysis (JEOL 2010, Tokyo, Japan, 120 keV) (see Figure S1 of the Supporting Information). On the basis of XPS analysis (see Figure S2 of the Supporting Information), the oxygen contents were 9.7% for the O-SWNTs and 5.7% for the SWNTs. The O functionalities consisted mostly of −COOH groups for the O-SWNTs and −COOH and −OH groups for the SWNTs (see Figure S2 of the Supporting Information). The presence of greater amounts of functional groups or amorphous carbon in the O-SWNTs than in the SWNTs was confirmed by TGA analysis, which revealed a higher mass loss for the O-SWNTs (see Figure S3 of the Supporting Information).[20]

Incubation of CNTs with Enzymes. Before incubation with LiP, 2 mg of SWNTs or O-SWNTs was added to 4.0 mL of citrate phosphate buffer (pH 4.6, 10 mM) and sonicated for 1 h in 15 min intervals in an ultrasonication bath (Branson Ultrasonic 5510, Danbury, CT, 40 kHz). Sonication did not significantly affect the CNT structure, as evidenced by the lack of structural changes in the control samples without enzymes. Lyophilized LiP was solubilized in citrate phosphate buffer at 0.03 units/mL, and 4.0 mL of this solution was added to the suspensions of SWNTs or O-SWNTs. An 8.0 mL volume of 80 μM H_2O_2 was added to the suspensions to give a total volume of 16.0 mL. LiP activity was determined on the basis of the removal of synthetic estrogen.[15] The vials were sealed with septa and wrapped with parafilm to create an airtight seal. An aliquot of 250 μL of 80 μM H_2O_2 was added to the vial daily for 2 weeks. All vials were covered with aluminum foil to avoid interference from photoreactions. The reaction vials were continuously stirred with magnetic stir bars. All experiments were performed in duplicate. Because of the continuous stirring and the surfactant effects of the proteins, the CNTs remained suspended in the solution and no obvious precipitation occurred. LiP activity was monitored every 2 days according to Srinivasan's method based on oxidation of veratryl alcohol.[21]

For incubations with MnP, the reaction medium (15 mL) contained 2 mg of SWNTs or O-SWNTs, 0.13 mM $MnSO_4$, 0.05 units/mL MnP, and 0.013 mM H_2O_2 in 50 mM sodium malonate buffer (pH 4.5). An aliquot of 250 μL of 0.013 mM H_2O_2 was added every 2 days for 2 weeks. MnP activity was determined and modified on the basis of the oxidation of phenanthrene.[22] The MnP activity was monitored using Srinivasan's method.[21]

For incubations with Lac, the medium (15 mL) contained 2 mg of SWNTs or O-SWNTs, 1 unit/mL Lac, and 50 μM ABTS in 50 mM sodium citrate buffer (pH 5.0). Lac activity was determined on the basis of the removal of polycyclic aromatic hydrocarbons.[23] The vial was loosely sealed to ensure sufficient oxygen in the system. Lac activity was monitored according to Canas' method.[23]

Characterization of CNT Structural Changes. Prior to Raman spectroscopy analysis, samples were centrifuged at 3100 *g* for 3 h and the supernatant was decanted to remove salts from the buffer. The samples were then resuspended in methanol by sonication with an ultrasonic homogenizer (Sonic Ruptor 250, Heat Systems Ultrasonic, Inc., Plainview, NY) at 80−100 W for 1 min. Samples were prepared by drop casting 20 μL of the suspension on a quartz microscope slide and air drying. All spectra were collected on an inVia Raman microscope (Renishaw, U.K.) at an excitation wavelength of 633 nm. Samples were scanned from 1000 to 1800 cm^{-1} to visualize the D- and G-band intensity changes during the degradation process. Spectra were collected with a 15 s exposure time and averaged across 5 scans per sample. To verify the structural changes, the enzymatic transformation of SWNTs by MnP was repeated in triplicate and additional Raman spectra were obtained (see Figure S4 of the Supporting Information). For NIR spectroscopy analysis, aqueous samples were diluted 10-fold and sonicated with an ultrasonic homogenizer (Sonic Ruptor 250) at 80−100 W for 1 min. The CNTs were scanned from 600 to 1300 nm using a UV−vis−NIR spectrophotometer (Varian 500, Palo Alto, CA). Prior to TEM analysis, 1 mL of the sample was centrifuged at 18700 *g* for 30 min and the supernatant was decanted to remove salts from the buffer. This centrifugation speed and duration enables collection of all nanoparticles, including those associated with enzymes, and is adequate to precipitate

dx.doi.org/10.1021/es5011175 | Environ. Sci. Technol. 2014, 48, 7918−7923

proteins. The sample was then resuspended in approximately 1 mL of methanol by sonication (Sonic Ruptor 250) at 80−100 W for 1 min. The suspensions were then diluted 10-fold to achieve appropriate concentrations for analysis. One drop of the prepared sample was placed on a lacey carbon grid (Electron Microscopy Sciences) and allowed to dry under ambient conditions for 2 h prior to TEM imaging (JEOL 2010, Tokyo, Japan, 120 keV).

RESULTS AND DISCUSSION

Degradation of SWNTs by MnP. The Raman spectra of the SWNTs and O-SWNTs after incubation with the three enzymes are compared in Figure 1. No structural changes were

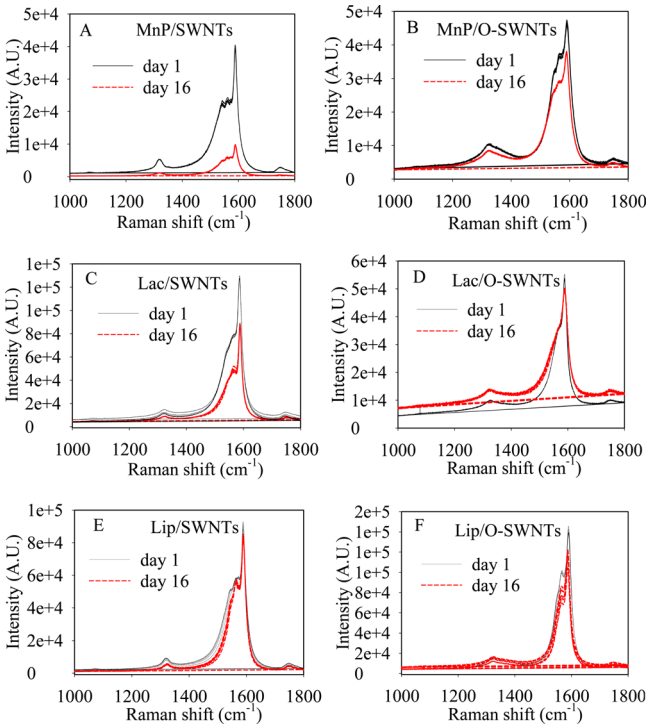

Figure 1. Raman spectra of the SWNTs and O-SWNTs incubated with different enzymes: (A) SWNTs treated with manganese peroxidase (MnP/SWNTs), (B) O-SWNTs treated with manganese peroxidase (MnP/O-SWNTs), (C) SWNTs treated with laccase (Lac/SWNTs), (D) O-SWNTs treated with laccase (Lac/O-SWNTs), (E) SWNTs treated with lignin peroxidase (Lip/SWNTs), and (F) O-SWNTs treated with lignin peroxidase (Lip/O-SWNTs).

observed in controls containing the same components (including H_2O_2, if added) but no enzymes after the 16 days of incubation. The activities of LiP and Lac decreased rapidly, and almost no activity was observed after the 10 days of incubation. MnP exhibited a slower decrease in activity than LiP over the 16 days of incubation period (see Figure S5 of the Supporting Information). Biotransformation was observed only for SWNTs exposed to MnP, as reflected by a dramatic decrease in the intensity of the G band and a significant increase ($p < 0.05$) in the D/G height ratio from 0.13 ± 0.03 (day 1) to 0.24 ± 0.02 (day 16). The tangential G band and disorder-induced D band are characteristic of graphitic carbon materials,[12] and the D/G height ratio is an index of structural disorder.[24] Therefore, the increase in the D/G height ratio of the SWNTs after MnP treatment indicates a significant increase in the number of holes and defects on the surfaces of the SWNTs.

In contrast, only small decreases in the intensities of the G and D bands were observed on the surfaces of the O-SWNTs (Figure 1B), and the D/G height ratio remained constant at 0.24 after the 16 days of incubation. This evidence indicates that no detectable structural alteration occurred on the surfaces of the O-SWNTs, in contrast to reports of complete O-SWNT degradation within 10 days when treated with HRP.[12,13] Whether this discrepancy is attributable to the lower redox potential of MnP (0.8 V)[25] compared to that of HRP (0.94−0.96 V)[26] remains to be determined.

Although decreases in the intensities of the G and D bands were observed for the SWNTs incubated with Lac (Figure 1C), the D/G height ratio remained relatively constant at 0.11. Similarly, no structural changes in the O-SWNTs were observed after 2 weeks of incubation with Lac (Figure 1D). Interestingly, although LiP and MnP are closely related enzymes with similar catalytic cycles, they exhibited different substrate specificities and LiP did not degrade SWNTs or O-SWNTs under the tested conditions (panels E and F of Figure 1).

The structural changes in the SWNTs treated with MnP were corroborated by the NIR spectra. Before incubation, the NIR absorption spectrum of the SWNTs showed sharp S2 (1000−1100 nm) and M1 (650−750 nm) bands, corresponding to semiconducting electronic and metallic properties, respectively (Figure 2A).[12] Upon incubation with MnP for 1

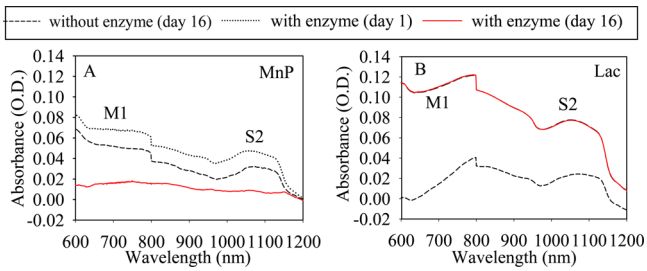

Figure 2. Vis−NIR spectra of the SWNTs before and after enzyme treatment: (A) MnP and (B) Lac. The spectrum of SWNTs treated with Lac on day 1 overlaps with the spectrum obtained on day 16.

day, the band shape and relative intensity of S2 and M1 remained unchanged and were essentially identical to those of the control. The increased absorption was likely due to the color change in the presence of enzymes (Figure 2A). Upon incubation with MnP for 16 days, both the S2 and M1 bands disappeared, indicating oxidative degradation of the graphitic structure. However, for the SWNTs incubated with Lac, the band shape and intensity of S2 and M1 were unchanged after the 16 days of incubation (Figure 2B). Thus, the NIR results confirm that, of the three ligninolytic enzymes, only MnP degraded the SWNTs.

Figure 3 shows TEM images of the SWNTs before (Figure 3A) and after (Figure 3B) MnP treatment, which reveal the morphological changes in the SWNTs that occurred upon incubation with the enzyme. In contrast, the SWNT tubular structure was maintained following Lac treatment (Figure 3C). Note that the high background concentration of carbon because of the malonate buffer masked the subtle mass change as a result of biotransformation, making it difficult to quantify the mass loss through total organic carbon or TGA analysis.

dx.doi.org/10.1021/es5011175 | Environ. Sci. Technol. 2014, 48, 7918−7923

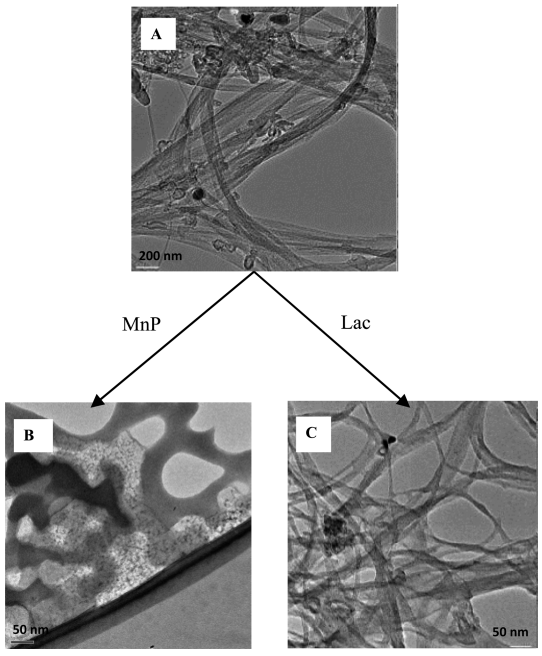

Figure 3. TEM images of the SWNTs: (A) before incubation with MnP, (B) after incubation with MnP for 16 days, showing the disappearance of the tubular structure, and (C) after incubation with Lac for 16 days, showing no loss of the tubular structure.

The biotransformation of O-SWNTs by MnP observed in this study contrasts the relative recalcitrance of O-SWNTs reported in the presence of a different peroxidase (HRP).[27] However, using HRP also, Allen et al.[12,13] observed significant structural changes of O-SWNTs after 10 days of incubation. Such discrepancies in biotransformation capabilities are common in the literature and may reflect differences in materials used (e.g., the CNTs are usually prepared by the testing laboratory and may exhibit differences in defects and amorphous carbon content) and reaction conditions (e.g., concentration of the enzyme and mediator).

Carboxyl Groups on the O-SWNTs May Interfere with the MnP Catalytic Cycle. It is commonly assumed that the structural defects associated with the formation of O-SWNTs and their closer orientation to the active sites of enzymes facilitate their biodegradation compared to SWNTs.[13,19] However, our observation that SWNTs are more susceptible to MnP transformation than O-SWNTs contradicts this notion and emphasizes the need to reconsider heuristic assumptions about the effects of the surface functionalization of SWNTs (particularly by carboxyl groups) on their susceptibility to biodegradation.

As shown in Figure 4, the catalytic cycle of MnP proceeds as follows: (i) H_2O_2 acts as the oxidizing substrate for MnP (reaction 1), resulting in the formation of compound **I** (two-electron oxidized enzyme); (ii) Mn^{2+} transfers one electron to compound **I** (reaction 2), reducing it to compound **II** and producing Mn^{3+}; and (iii) Mn^{2+} transfers a second electron to compound **II** (reaction 3), reducing the enzyme back to MnP and producing another Mn^{3+}. Produced Mn^{3+} is very unstable and can readily complex with carboxylic acids (e.g., malonate in this study). Mn^{3+} malonate is a strong oxidant that can either react directly with SWNTs or react through malonate-mediated oxidation. We postulate that the small degree of hydroxylation of the SWNT surfaces may facilitate direct oxidation because

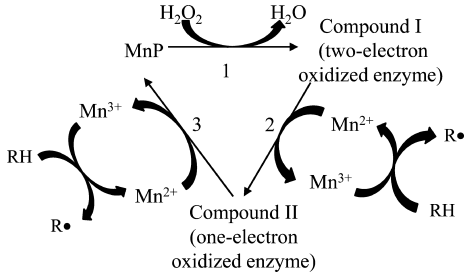

Figure 4. Catalytic cycle of MnP, showing three reactions. RH and R• represent various substrates and related radicals.

the hydroxylated surface reassembles phenolic (hydroxylated) lignin compounds, which are the primary substrate for MnP.[28] For malonate-mediated oxidation, malonate can be oxidized by Mn^{3+} in the presence of O_2 to produce radicals (e.g., alkyl peroxyl radicals, superoxide, and formate radicals),[28] which can attack SWNTs non-specifically.

The lack of biodegradation of the O-SWNTs is likely attributable to the interference of the carboxyl groups with the Mn^{2+}/Mn^{3+} catalytic cycle. First, by binding Mn^{2+} at the binding site of the enzyme, the carboxyl groups on the O-SWNTs interfere with the oxidation of Mn^{2+} to Mn^{3+}, subsequently interrupting the enzymatic cycle. Generally, the binding ligands (carboxyl groups) for Mn^{2+} in MnP are Asp179, Glu35, and Glu39 (Figure 5A).[29,30] However, when CNTs are in proximity to the binding site, coordination binding between the carboxylated CNTs and Mn^{2+} likely occurs because carboxylated CNTs can form strong complexes with divalent metals, such as Cu^{2+}, Pb^{2+}, Zn^{2+}, and Co^{2+}.[31] Such complex

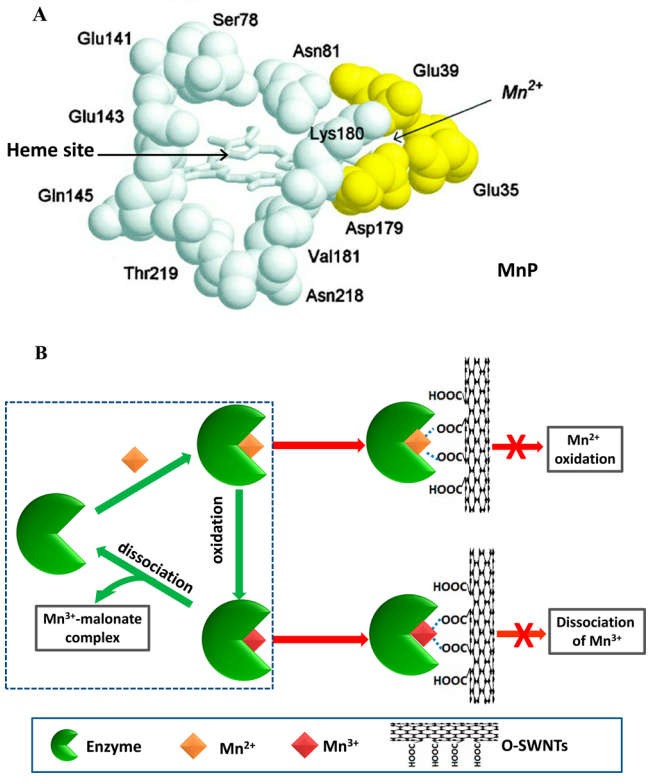

Figure 5. Illustration of the (A) heme site and Mn-binding site inside MnP (adapted with permission from ref 29) and (B) interference of the O-SWNTs with the Mn^{2+}/Mn^{3+} catalytic cycle.

dx.doi.org/10.1021/es5011175 | Environ. Sci. Technol. 2014, 48, 7918−7923

formation may hinder the oxidation of Mn^{2+} (Figure 5B). Second, Mn^{3+} must complex with malonate to dissociate from the enzyme, but if Mn^{3+} forms a complex with the carboxylated CNTs at the binding site, the formation of the Mn^{3+}−malonate complex will be inhibited. Thus, Mn^{3+} could not easily dissociate from the enzyme, and the enzymatic cycle could not be completed (Figure 5B).

Note that SWNTs also contain some carboxyl functionality, making them susceptible to the proposed inhibitory mechanism (i.e., complexation between carboxylated CNTs and Mn^{2+} and/or Mn^{3+}). We propose that the different degradability of the SWNTs and O-SWNTs is attributable to their different degrees of carboxylation (see Figures S2 and S3 of the Supporting Information). To form coordination bonds, the distance between Mn^{2+} and carboxyl oxygen must be within the hydrogen-bonding distance. Therefore, only when CNTs are in the proximity of the Mn^{2+}/Mn^{3+} binding site can they interfere with the Mn^{2+}/Mn^{3+} cycle. In comparison to SWNTs, O-SWNTs can approach closer to the binding site of MnP. On the basis of the results of molecular modeling, Allen et al.[13] proposed that O-SWNTs can position at the active site more easily than SWNTs because of interactions between negatively charged carboxyl groups (on O-SWNTs) and positively charged residues (Arg178 on HRP). Similarly, in the present study, the carboxyl groups of O-SWNTs likely interacted with the positively charged residues His46 and Arg42 (which form the peroxide binding pocket of MnP[32]), resulting in a closer orientation to the MnP binding site (Figure 5A) than that of SWNTs.

The lack of degradation of O-SWNTs observed in this study was not caused by complexation between the O-SWNTs and Mn^{2+} in solution (although the O-SWNTs could also theoretically interrupt the enzymatic cycle of MnP by decreasing free Mn^{2+} in solution). Under the experimental conditions, the O-SWNTs adsorbed less than 10% of the total Mn^{2+} added (see Figure S6 of the Supporting Information). The low adsorption capacity of the O-SWNTs for Mn^{2+} is likely due to the presence of malonate and Na^{+}, which might compete with CNTs for Mn^{2+} or occupy adsorption sites on the CNTs.

Overall, contrary to common wisdom, these mechanistic considerations suggest that carboxylation on SWNT surfaces may hinder biotransformation by some extracellular enzymes, such as MnP.

■ ASSOCIATED CONTENT

Supporting Information

TEM images of the SWNTs and O-SWNTs (Figure S1), XPS plots of the C 1s and O 1s core levels of the SWNTs and O-SWNTs (Figure S2), TGA plots of the SWNTs and O-SWNTs (Figure S3), additional Raman spectra of MnP treatments in triplicate (Figure S4), activities of the three enzymes during the 16 days of incubation (Figure S5), and adsorption of Mn^{2+} by the SWNTs and O-SWNTs (Figure S6). This material is available free of charge via the Internet at http://pubs.acs.org.

■ AUTHOR INFORMATION

Corresponding Authors

*Telephone: 86-22-6229517. E-mail: zhangchengdong@nankai.edu.cn.

*Telephone: 713-348-5903 and/or 713-348-5203. E-mail: alvarez@rice.edu.

Notes

The authors declare no competing financial interest.

■ ACKNOWLEDGMENTS

This work was supported by the National Science Foundation of China (Grants 81250003 and 81373039), the Ministry of Science and Technology (Grant 2014CB932001), and the China−U.S. Center for Environmental Remediation and Sustainable Development.

■ REFERENCES

(1) Dresselhaus, M. S.; Dresselhaus, G.; Jorio, A. Unusual properties and structure of carbonnanotubes. *Annu. Rev. Mater. Res.* **2004**, *34*, 247−278.

(2) Bandaru, P. R. Electrical properties and applications of carbon nanotube structures. *J. Nanosci. Nanotechnol.* **2007**, *7* (4−5), 1239−1267.

(3) Harrison, B. S.; Atala, A. Carbon nanotube applications for tissue engineering. *Biomaterials* **2007**, *28* (2), 344−353.

(4) Malarkey, E. B.; Parpura, V. Applications of carbon nanotubes in neurobiology. *Neurodegener. Dis.* **2007**, *4* (4), 292−299.

(5) Mauter, M. S.; Elimelech, M. Environmental applications of carbon-based nanomaterials. *Environ. Sci. Technol.* **2008**, *42* (16), 5843−5859.

(6) Shannon, M. A.; Bohn, P. W.; Elimelech, M.; Georgiadis, J. G.; Mariñas, B. J.; Mayes, A. M. Science and technology for water purification in the coming decades. *Nature* **2008**, *452* (7185), 301−310.

(7) Jia, G.; Wang, H. F.; Yan, L.; Wang, X.; Pei, R. J.; Yan, T.; Zhao, Y. L.; Guo, X. B. Cytotoxicity of carbon nanomaterials: Single-wall nanotube, multi-wall nanotube, and fullerene. *Environ. Sci. Technol.* **2005**, *39* (5), 1378−1383.

(8) Kang, S.; Mauter, M. S.; Elimelech, M. Microbial cytotoxicity of carbon-based nanomaterials: Implications for river water and wastewater effluent. *Environ. Sci. Technol.* **2009**, *43* (7), 2648−2653.

(9) Maynard, A. D.; Aitken, R. J.; Butz, T.; Colvin, V.; Donaldson, K.; Oberdorster, G.; Philbert, M. A.; Ryan, J.; Seaton, A.; Stone, V.; Tinkle, S. S.; Tran, L.; Walker, N. J.; Warheit, D. B. Safe handling of nanotechnology. *Nature* **2006**, *444* (7117), 267−269.

(10) Petersen, E. J.; Zhang, L.; Mattison, N. T.; O'Carroll, D. M.; Whelton, A. J.; Uddin, N.; Nguyen, T.; Huang, Q.; Henry, T. B.; Holbrook, R. D.; Chen, K. L. Potential release pathways, environmental fate, and ecological risks of carbon nanotubes. *Environ. Sci. Technol.* **2011**, *45* (23), 9837−9856.

(11) Liwen, Z.; Qingguo, H. Environmental fate, transport, and transformation of carbon nanoparticles. In *Biotechnology and Nanotechnology Risk Assessment: Minding and Managing the Potential Threats around Us*; Ripp, S., Henry, T. B., Eds.; American Chemical Society (ACS): Washington, D.C., 2011; Vol. *1079*, Chapter 4, pp 69−101.

(12) Allen, B. L.; Kichambare, P. D.; Gou, P.; Vlasova, I. I.; Kapralov, A. A.; Konduru, N.; Kagan, V. E.; Star, A. Biodegradation of single-walled carbon nanotubes through enzymatic catalysis. *Nano Lett.* **2008**, *8* (11), 3899−3903.

(13) Allen, B. L.; Kotchey, G. P.; Chen, Y. N.; Yanamala, N. V. K.; Klein-Seetharaman, J.; Kagan, V. E.; Star, A. Mechanistic investigations of horseradish peroxidase-catalyzed degradation of single-walled carbon nanotubes. *J. Am. Chem. Soc.* **2009**, *131* (47), 17194−17205.

(14) Kagan, V. E.; Konduru, N. V.; Feng, W. H.; Allen, B. L.; Conroy, J.; Volkov, Y.; Vlasova, I. I.; Belikova, N. A.; Yanamala, N.; Kapralov, A.; Tyurina, Y. Y.; Shi, J. W.; Kisin, E. R.; Murray, A. R.; Franks, J.; Stolz, D.; Gou, P. P.; Klein-Seetharaman, J.; Fadeel, B.; Star, A.; Shvedova, A. A. Carbon nanotubes degraded by neutrophil myeloperoxidase induce less pulmonary inflammation. *Nat. Nanotechnol.* **2010**, *5* (5), 354−359.

(15) Mao, L.; Huang, Q. G.; Lu, J. H.; Gao, S. X. Ligninase-mediated removal of natural and synthetic estrogens from water: I. Reaction behaviors. *Environ. Sci. Technol.* **2009**, *43* (2), 374−379.

(16) Colosi, L. M.; Burlingame, D. J.; Huang, Q. G.; Weber, W. J. Peroxidase-mediated removal of a polychlorinated biphenyl using natural organic matter as the sole cosubstrate. *Environ. Sci. Technol.* **2007**, *41* (3), 891−896.
(17) Haritash, A. K.; Kaushik, C. P. Biodegradation aspects of polycyclic aromatic hydrocarbons (PAHs): A review. *J. Hazard. Mater.* **2009**, *169* (1−3), 1−15.
(18) Schreiner, K. M.; Filley, T. R.; Blanchette, R. A.; Bowen, B. B.; Bolskar, R. D.; Hockaday, W. C.; Masiello, C. A.; Raebiger, J. W. White-rot basidiomycete-mediated decomposition of C_{60} fullerol. *Environ. Sci. Technol.* **2009**, *43* (9), 3162−3168.
(19) Liu, X.; Hurt, R. H.; Kane, A. B. Biodurability of single-walled carbon nanotubes depends on surface functionalization. *Carbon* **2010**, *48* (7), 1961−1969.
(20) McPhail, M. R.; Sells, J. A.; He, Z.; Chusuei, C. C. Charging nanowalls: Adjusting the carbon nanotube isoelectric point via surface functionalization. *J. Phys. Chem. C* **2009**, *113* (32), 14102−14109.
(21) Srinivasan, C.; Dsouza, T. M.; Boominathan, K.; Reddy, C. A. Demonstration of laccase in the white rot basidiomycete *Phanerochaete chrysosporium* BKM-F1767. *Appl. Environ. Microb.* **1995**, *61* (12), 4274−4277.
(22) Hammel, M. A. M. K. E. Lipid peroxidation by the manganese peroxidase of *Phanerochaete chrysosporium* is the basis for phenanthrene oxidation by the intact fungus. *Appl. Environ. Microbiol.* **1994**, *60* (6), 1956−1961.
(23) Canas, A. I.; Alcalde, M.; Plou, F.; Martinez, M. J.; Martinez, A. T.; Camarero, S. Transformation of polycyclic aromatic hydrocarbons by laccase is strongly enhanced by phenolic compounds present in soil. *Environ. Sci. Technol.* **2007**, *41* (8), 2964−2971.
(24) Bissett, M. A.; Shapter, J. G. Photocurrent response from vertically aligned single-walled carbon nanotube arrays. *J. Phys.Chem. C* **2010**, *114* (14), 6778−6783.
(25) Singh, S. N. *Microbial Degradation of Xenobiotics*; Springer: Heidelberg, Germany, 2012.
(26) Kotchey, G. P.; Hasan, S. A.; Kapralov, A. A.; Ha, S. H.; Kim, K.; Shvedova, A. A.; Kagan, V. E.; Star, A. A natural vanishing act: The enzyme-catalyzed degradation of carbon nanomaterials. *Acc. Chem. Res.* **2012**, *45* (10), 1770−1781.
(27) Flores-Cervantes, D. X.; Maes, H. M.; Schäffer, A.; Hollender, J.; Kohler, H.-P. E. Slow biotransformation of carbon nanotubes by horseradish peroxidase. *Environ. Sci. Technol.* **2014**, *48* (9), 4826−4834.
(28) Hofrichter, M. Review: Ligin conversion by manganese peroxidase (MnP). *Enzyme. Microb. Technol.* **2002**, *30*, 454−466.
(29) Harris, R. Z.; Wariishi, H.; Gold, M. H.; Ortiz de Montellano, P. R. The catalytic site of manganese peroxidase. Regiospecific addition of sodium azide and alkylhydrazines to the heme group. *J. Biol. Chem.* **1991**, *266* (14), 8751−8758.
(30) Camarero, S. Description of a versatile peroxidase involved in the natural degradation of lignin that has both manganese peroxidase and lignin peroxidase substrate interaction sites. *J. Biol. Chem.* **1999**, *274* (15), 10324−10330.
(31) Pyrzynska, K. Carbon nanostructures for separation, preconcentration and speciation of metal ions. *TrAC, Trends Anal. Chem.* **2010**, *29* (7), 718−727.
(32) Sundaramoorthy, M.; Kishi, K.; Gold, M. H.; Poulos, T. L. The crystal structure of manganese peroxidase from *Phanerochaete chrysosporium* at 2.06-Å resolution. *J. Biol. Chem.* **1994**, *269* (52), 32759−32767.